

# Experimental Study of New Generation WWER-1000 Fuel Assemblies at JSC NCCP

A. Enin, V. Rozhkov, Y. Sinikov, A. Ustimenko, M. Shustov

JSC NCCP, Novosibirsk, Russian Federation

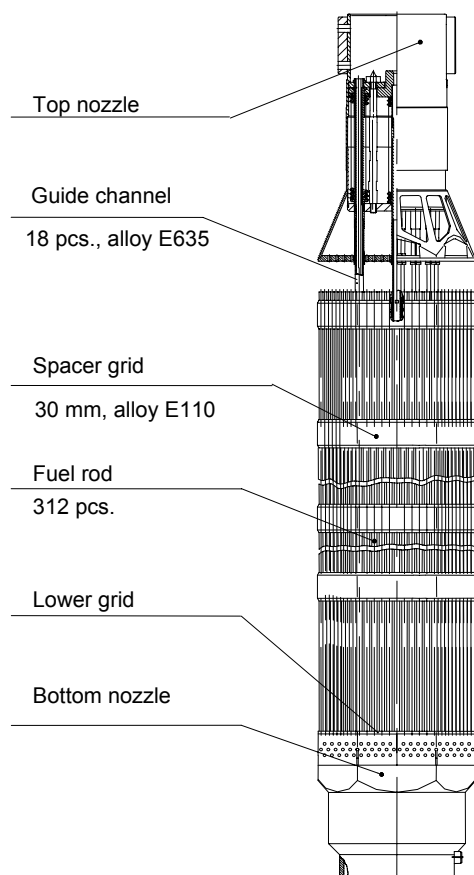


Figure 1. TVS-2 fuel assembly

## 1. Introduction

Expansion of the Russian nuclear fuel market and increase of nuclear fuel competitiveness require development of fuel assemblies (FAs) with improved operational characteristics. Serial WWER-1000 FA is a multi fuel rod (FR) design in which fuel rods and guide channels (GC) are arranged in

a bundle by means of spacer grids (SG). One of technical requirements to new FA design types is resistance to deformation within five and more years of in-core operation. The resistance to deformation is achieved thanks to development of new generation FAs with rigid carrying skeleton.

At the stage of technical offer in 1999-2000 together with the RF State Scientific Center (SSC) Institute of Physics and Power Engineering (IPPE), FA thermomechanical stability conception [1] was formulated and development of design code prototypes began. During preliminary calculation the requirements to new design rods were determined:

- Material and geometrical dimensions of spacer grid cells;
- SG quantity;
- Material and GC geometrical dimensions;
- Method of SG to GC fastening.

The present stage resulted in offer of FA design.

But the analysis of FA and reactor core design strength and thermomechanical properties is rather sophisticated task that's why at the beginning of technical project the program of experimental study of FA thermomechanical stability was established together with RF SSC IPPE and Russian Scientific Center Kurchatov Institute. The program was aimed at the following:

- More precise specification of design;
- Verification of design models and codes;
- Substantiation of design element strength and rigidity;
- Substantiation of FA serviceability during FR bundle-skeleton interaction.

For tests the assembly fragments and small dummy models of FA skeletons and FR bundles were used. This made it possible to conduct the comparison experiments and determine the required mechanical characteristics of different design modifications with small expenses.

Table 1. Characteristics of SGs

Type	Height, [mm]	Cell wall thickness, [mm]	Dimple length, [mm]	Welding
A (SG of serial FA)	20	0.25	12	GC - cell
B	30	0.25	24	GC - cell
C	30	0.25	24	GC-bushing-cell
D	30	0.30	24	GC - cell
E(TVS-2)	30	0.30	4	GC - cell

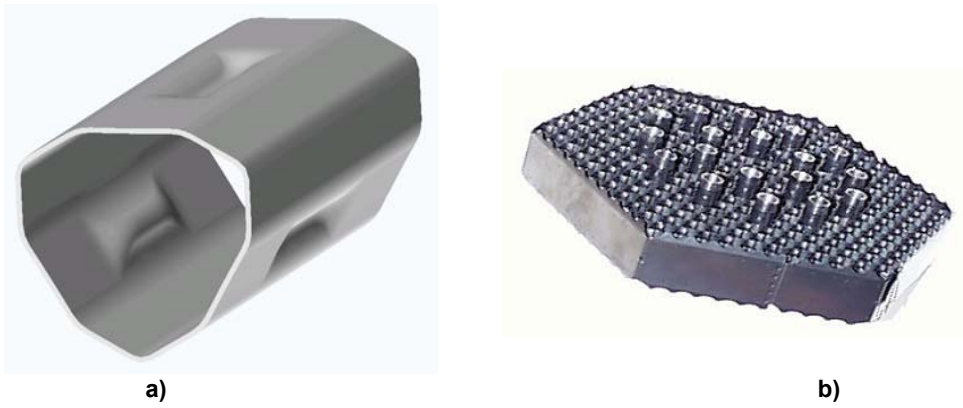


Figure 2. E-type cell (a) and spacer grid with welded guide channels (b)

## 2. Design Features and Composition of Tests

Tests were conducted during design of FA, the so-called TVS-2, with rigid skeleton in which zirconium alloy GCs are joined with zirconium alloy SG cells by resistance-butt welding. Sketch of TVS-2 is presented in Figure 1. Characteristics of SGs that were used for tests are given in Table 1, the cell and spacer grid are given in Figure 2.

The tests were conducted using tensile-testing machine. Measurement error didn't exceed 1%. Movement speed was 0.5 or 1.0 mm/min. Machining attachments used during tests provided for self-deformation not exceeding 3% of the measured movements. If it was impossible to provide for the required rigidity, the calibration tests were conducted, and during data processing the machining attachment yielding was taken into consideration. All tests were performed at room temperature.

During experimental data processing the statistical methods were used. The following assumptions were made: 0.95 confidence level, 0.05 rare event significance level, estimate of upper and lower bounds. Linear regression was estimated by the least square method. Estimation of difference of regression line slopes was made by Student t-criterion.

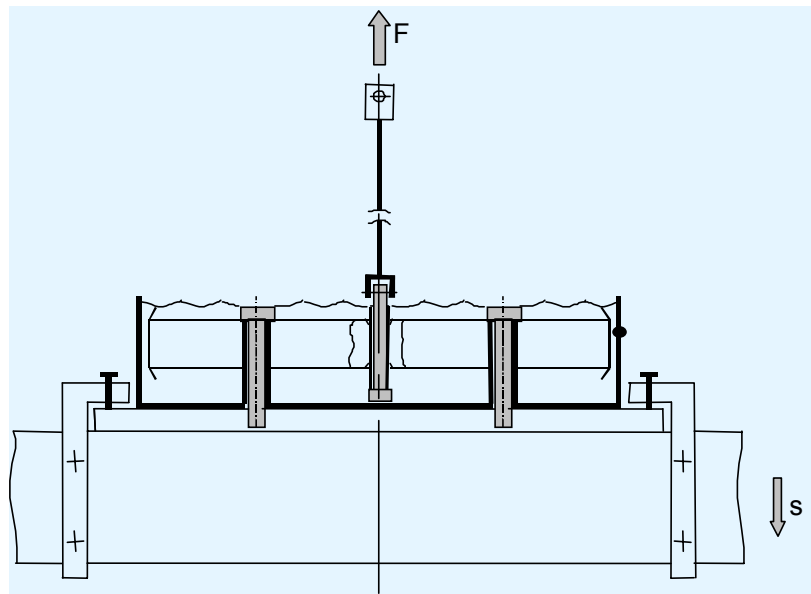


Figure 3. Scheme of FR dragging through spacer grid

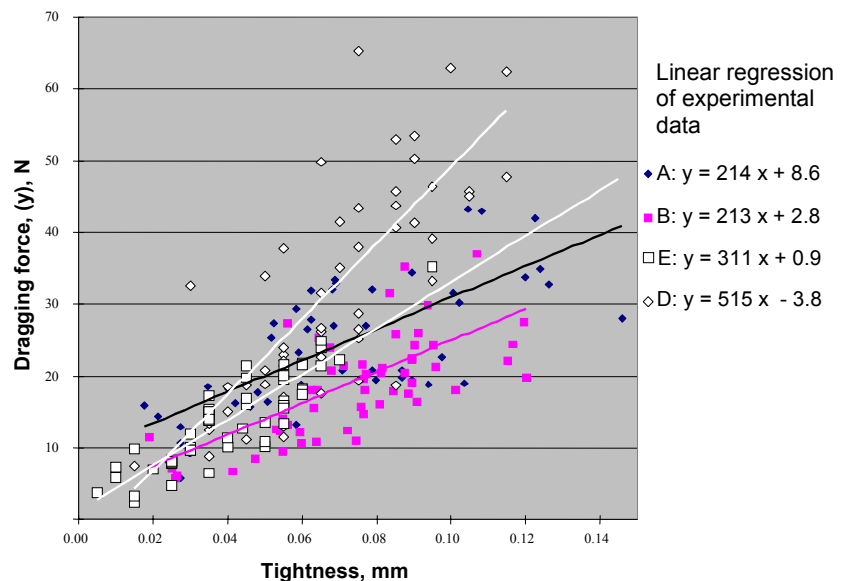


Figure 4. Test results on FR dragging through spacer grid

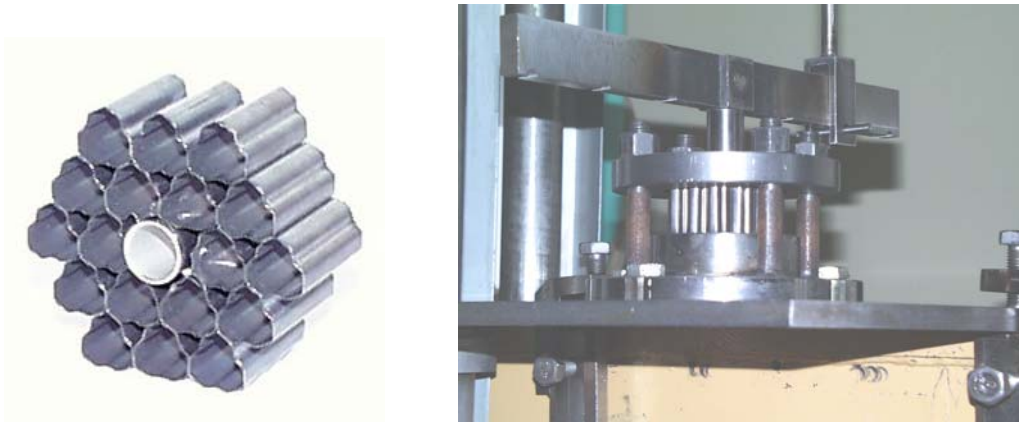


Figure 5. Fastening unit and attachments for tests of GC rotation in spacer grid

### 3. Results of SG and Fastening Units Testing

FR dragging through SG cells was performed according to the scheme given in Figure 3 (in air and in water) and “s movement - F force” diagrams were recorded.

It was assumed that dragging force ( $y$ ) is in direct proportion to tightness ( $x$ ) in FR-cell pair, i.e. regression line slope is in direct proportion to cell rigidity in case of dimple radial deformation. Comparison of data obtained under different test conditions consisted in check of statistical hypothesis of equality of regression line slopes. Test results are given in Figure 4. No dependence of dragging force on the cell position in spacer grid and the environment (water or air) in which the tests were performed was detected. Regression lines recorded based on experimental data differ considerably for types A, D and E.

Non-zero free term of regression equation results from misalignment of dragging force and cell axes during the tests (Figure 3). Only for E-type cells, free term insignificantly differs from zero, i.e. force of FR dragging through TVS-2 spacer grid is low sensitive to FR rotation.

FR rotation in the SG cell was performed about two perpendicular axis. During the tests it was found that in case of FR rotation in the cell, “movement  $s$  – force  $F$ ” diagram is characterized by the areas that make it possible to determine the following:

- Limit angle of FR elastic rotation in the cell that corresponds to the beginning of non-linear area of loading diagram;
- Rigidity for FR rotation angle less than limit an-

gle of FR elastic rotation;

- Rigidity for FR rotation angle  $\sim 0.6^\circ$ .

The tests showed that the limit angle of FR elastic rotation in the cell when the friction forces deform the cell without FR movement relative to dimple is very small. With increase of FR rotation angle the FR is moved relative to cell dimple and rotation rigidity decreases abruptly - nearly 5 times. SGs with short dimple have the lowest rotation rigidity.

Experiments of GC rotation and push through were conducted with fastening unit specimens using special attachments (Figure 5). The specimens consisted of 18 cells with welded GC simulator.

GC rotation was made similar to FR rotation in SG in two perpendicular directions. No statistically significant rigidity differences were detected during rotation about the mentioned axes.

The rigidity for rotation angles in the range of  $0 \dots 0.1^\circ$  and rigidity for  $\sim 0.6^\circ$  rotation angle were determined, the obtained values differed from each other considerably. No rigidity dependence on quantity of loading cycles was observed.

C-type fastening unit welded using intermediate bushing has the lowest rotation rigidity. Strength and rigidity of GC-to-SG fastening unit increases more than two times with increase of cell wall thickness from 0.25 to 0.30 mm and height increase from 20 to 30 mm. Fastening unit E (TVS-2) has the highest strength and rigidity.

Analysis of the push through force and the rigidity during FR rotation in the SG cell made it possible to identify the interaction mechanisms in FR-cell pair and to make choice for the benefit of E-type cell (with short dimple). Actual rigidity values for GC rotation in SG were used for more precise definition of design codes for thermomechanical FA and reactor core (as a whole) behaviour.

During the test by pushing one GC through SG it was found that destruction of fastening unit occurs because of weld spot tearing from SG cells.

Table 2. Results of pushing one GC through SG

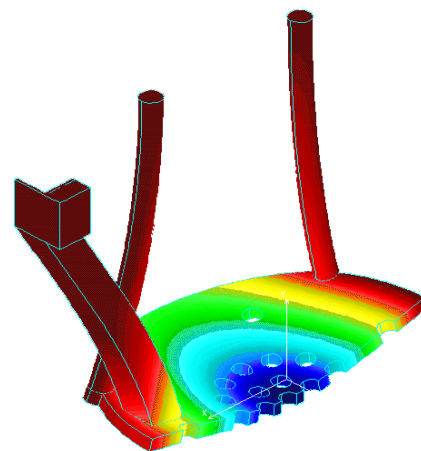
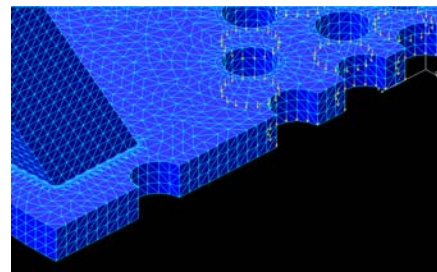
Type	A	B	C	E
Average destruction force, [kN]	4.1	5.3	5.1	11.3

**Table 3. Dummy models of skeletons and FR bundles**

Type	Skeleton	SG span, [mm]	
A1f	friction	255	 <p>Welded skeleton dummy model</p>
A2f	friction	285	
B1f	friction	250	
B2f	friction	280	
B2f	friction	280	
A1	welding	255	
A2	welding	285	
B1	welding	250	
B2	welding	280	
C1	welding, bushing	250	
E2	welding	280	
bA1	welding	255	9.115
bA2	welding	285	9.125
bB1	welding	250	9.125
bB2	welding	280	9.125
bB1	welding, bushing	250	9.115
bE2	welding	280	9.125



a)



b)

**Figure 6. Cage for skeleton and bundle dummy model tests: a) – general view; b) – finite-element model and mounting deformation calculation**

Specimens of 20 mm height were destroyed with considerable turn of axis of cells adjoining GC and specimen warping. Test results are given in Table 2.

During SG compression test in the plane the elastic deformation limit and force above which the

SG lost its carrying capacity were recorded. Comparison of A and E spacer grids shows more than three times greater SG strength and rigidity in case of increase of cell wall from 0.25 to 0.30 mm and increase of cell height from 20 to 30 mm.

The obtained test results of FA units and parts strength made it possible to decrease the conservative margins of FA strength estimate during operation.

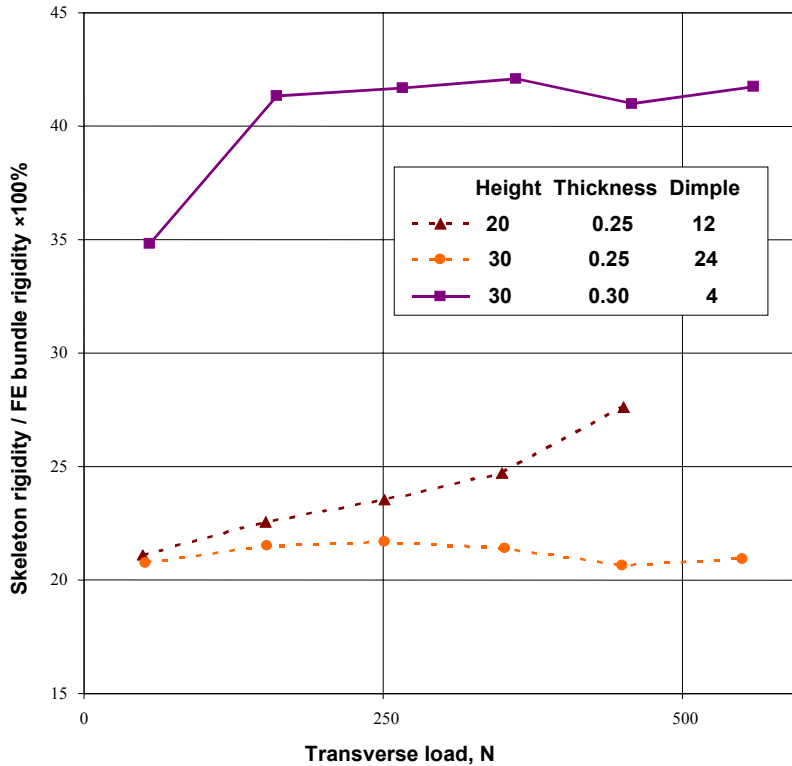


Figure 7. Skeleton rigidity- FR bundle rigidity proportion

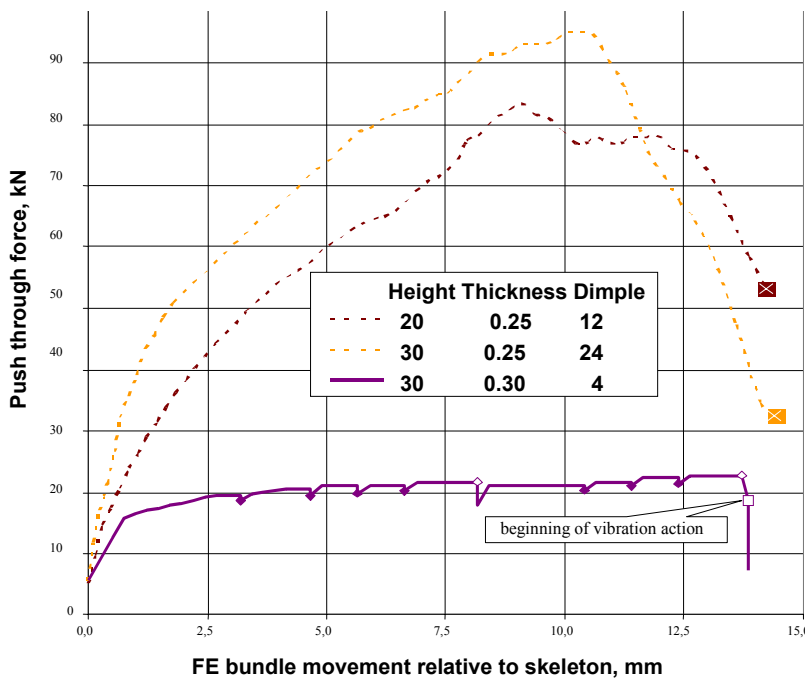


Figure 8. Results of FR bundle dummy model push through tests; on the curves the points of loading and unloading in transverse direction and points of destruction are marked

#### 4. Results of Skeleton and FR Bundles Dummy Model Bend Tests

Dummy models of skeletons and FR bundles containing three spacer grids each were fabricated according to Table 3 and tested in the special device (cage). The cage design makes it possible to apply a transverse force to the middle SG of dummy model as well as to push FR simulator bundle through the stationary skeleton by means of tensile-testing machine.

During cage design the finite rod method that made it possible to account for cage deformation during tests was used (Figure 6).

Skeleton and FR bundle rigidity was determined by means of bend tests. Analysis of test results showed the following:

- Rigidity of skeleton dummy models assembled by friction decreases ~3 times with load increase from 50 to 500 N and has only a slight dependence on height and span of spacer grids;
- Rigidity of welded skeleton dummy models under the load 50 N is higher than the ones assembled by friction and slightly decreases (by 5...20%) with load increase from 50 to 1000 N;
- Rigidity of welded skeleton dummy models with 20 mm high SG is 20...30% lower than the one of 30 mm high SG;
- Rigidity of FR bundle

dummy models decreases by 20...45% with load increase 50-500 N;

- Rigidity of FR bundle dummy models depends on geometrical parameters of FR-cell pair, tightness and dimple length. The greatest rigidity has the FR bundle dummy model with 24 mm dimple length, containing FRs with the greatest average diameter (9.125 mm).

Welded skeleton with E-type SG provides the greatest fraction of FR bundle rigidity (Figure 7).

## 5. Test Results of FR Bundle Pushing through Skeleton with Simulation of FR Bundle Bending

FA thermomechanical behaviour was estimated during FR dummy model tests conducted by means FR bundle pushing through skeleton. The present tests simulated the FR bundle-with-skeleton interaction during transient operating conditions. Analysis of results presented in Figure 8 showed the following:

- Two dummy models with 20 mm high spacer grid were destroyed without transverse bending due to FR jamming in SG cells;
- One dummy model with 30 mm high spacer grid was destroyed without transverse bending due to FR jamming in SG cells; two dummy models of 30 mm high spacer grid were destroyed after applying of transverse load;
- In dummy models with 20 mm high SG, jamming is typical for FRs positioned near the SG corners. After destruction, SG surface has a form of lens; warping of SG inside the area enclosed by twelve external GCs is negligible. Concerning dummy models of all types, SG destruction occurs along cell-cell and cell-GC weld joints forming external contour of 12 GCs.

When testing the dummy models with 30 mm high SG, slight FR bundle movement is observed near

SG corners. After destruction SG surface has a conical form. SG warping inside the contour defined by external 12 guide channels is absent, within the mentioned contour (area) the FRs move without jamming.

Dummy model with SG of 30 mm height of E type (TVS-2) wasn't destroyed after applying of transverse load and 3.3 mm bending along the middle SG. After stop of traverse of tensile-testing machine and removal of transverse load applied to middle SG, the dummy model was subjected to vibration action that resulted in FR bundle movement relative to welded skeleton and the force decreased down to ~8000 N.

## 6. Conclusions

The test results are used for selection of design, verification of design codes and substantiation of operating capacity of FA with rigid skeleton:

Mechanical characteristics of units made it possible to perform FA strength and rigidity calculations, including the cases of abnormal operation;

Mechanical characteristics of skeleton and FR bundle dummy models made it possible to check for FA design model adequacy;

Mechanical characteristics of skeleton and FR bundle dummy models obtained during FR bundle push through experiments made it possible to substantiate the FA serviceability under the conditions of FR bundle and skeleton interaction.

## Reference

- [1] V. Troyanov, Y. Likhachev, V. Folomeev. General Study Statement on Thermomechanical Behaviour of the VVER-1000 Reactor Core. *Izvestia visshikh uchebnykh zavedeniy, Communications of Higher Schools, Nuclear Power Engineering*, 2, 33-43, 2002.